

---

LABORATORY INVESTIGATION

---

## Relationship Between the s-wave Amplitude of the Multifocal Electroretinogram and the Retinal Nerve Fiber Layer Thickness in Glaucomatous Eyes

Junfuku Nitta, Yutaka Tazawa, Ken-ichi Murai, Isao Egawa,  
Takashi Nabeshima, Tomoko Endo, Michiko Tanaka,  
and Shigeki Machida

Department of Ophthalmology, Iwate Medical University School of Medicine, Morioka, Japan

---

### Abstract

**Purpose:** To determine whether a significant correlation exists between the amplitude of the s wave of the multifocal electroretinogram (mfERG) and the retinal nerve fiber layer thickness (RNFLT) in glaucomatous eyes.

**Methods:** Twenty-three eyes of 23 patients with glaucoma were studied. In all eyes, the severity of the defects in the upper visual field differed significantly from the severity of those in the lower half. Patients having visual field halves with mean deviation (MD) values lower than -5 dB were placed in group A, and patients having visual field halves with MD values greater than -5 dB were placed in group B. The mfERGs were elicited by 37 stimulus elements alternating from white to black in a pseudorandom binary m-sequence at a frequency of 9.4 Hz. The mfERGs in the upper and lower visual field halves were summed to yield upper and lower averaged waves. The GDx variable corneal compensator and optical coherence tomography were used to measure the RNFLT.

**Results:** The retinal nerve fiber layer was significantly thinner in group A than in group B. There was a significant correlation between the RNFLT and the MD values of visual field defects. The s-wave amplitude was significantly smaller in group A than in group B. The s-wave amplitude also correlated significantly with the MD and the RNFLT.

**Conclusion:** The significant correlations between the s-wave amplitude and the MD, and between the S-wave amplitude and the RNFLT, indicate that the s-wave receives significant contributions from the retinal ganglion cells and their axons. **Jpn J Ophthalmol** 2005;49:481-490 © Japanese Ophthalmological Society 2005

**Key Words:** ganglion cell, glaucoma, multifocal electroretinogram, retinal nerve fiber layer thickness, s-wave

---

### Introduction

A small positive wave, the s-wave, is present on the descending limb of the first positive wave (P1) of a first-order kernel of a multifocal electroretinogram (mfERG) when the mfERG is recorded by a low stimulus frequency.<sup>1</sup> The amplitude of the s-wave increases and the implicit time

shortens as the distance decreases between the optic nerve head and the retina locus from which the s-wave was recorded.<sup>1</sup> This suggests that the s-wave is related to the neural activity of retinal ganglion cells (RGCs) or their axons. In support of this hypothesis, the amplitude of the s-wave in patients with optic neuritis was greatly reduced or absent, and the amplitude returned to normal levels when the optic neuritis was resolved.<sup>1</sup> In addition, the amplitude of the s-wave obtained from eyes with primary open-angle glaucoma (POAG) was significantly smaller than that obtained from normal eyes.<sup>2</sup> In normal eyes, the mean amplitude and implicit times of the s-wave in the upper visual field did not differ significantly from those in the

---

Received: December 9, 2004 / Accepted: January 8, 2005

Correspondence and reprint requests to: Yutaka Tazawa, Department of Ophthalmology, Iwate Medical University School of Medicine, 19-1 Uchimarui, Morioka 020-8505, Japan  
e-mail: drtea66ptnd@aol.com

lower visual field.<sup>3</sup> However, in glaucomatous eyes, the s-wave amplitude was significantly smaller in areas where the visual field defect was more severe.<sup>3</sup> When tetrodotoxin (TTX) and *N*-methyl-D-aspartate (NMDA), which are known to suppress RGCs and amacrine cells, were injected into the vitreous cavity of cat eyes, the s-wave disappeared (unpublished data). All of these observations strongly support the suggestion that the s-wave reflects the activity of the RGCs and their axons.

Several reports on mfERG waves that resemble the s-wave in wave shape have been made, including reports on the optic nerve head component<sup>4,5</sup> and the mfERG waves of glaucomatous eyes.<sup>6</sup> These waves were recorded at a stimulation frequency of 75 Hz, but we have determined in our laboratory that the s-wave is more prominent when the stimulation frequency is low. Therefore, the s-wave-like patterns reported by other investigators may be different from the s-wave described here.

The purpose of this study was to test our hypothesis that the s-wave reflects the neural activity of the RGCs and their axons. To test this hypothesis, we analyzed the s-waves recorded from glaucomatous eyes that had visual field defects with the severity of the defects varying significantly between the upper and the lower half of the visual field. The retinal nerve fiber layer thickness (RNFLT) was measured with the GDx variable corneal compensator (GDx) and by optical coherence tomography (OCT), and the correlation between the s-wave amplitude and RNFLT was also calculated. The purpose of this study was not to compare the measurement methods of the RNFLT by GDx and OCT; we used both GDx and OCT to confirm the RNFLT measurement.

## Subjects and Methods

### Subjects

The subjects were patients with glaucoma whose visual field defects in the upper field were significantly different from those in the lower field, as determined by a Humphrey field analyzer (HFA). Twenty-three eyes of 23 patients, consisting of 17 eyes of 17 patients with normal tension glaucoma (NTG) and 6 eyes of 6 patients with primary open-angle glaucoma (POAG), were studied. All subjects were being treated in our hospital at the time of enrollment in the study. There were 6 men and 17 women, whose ages ranged from 51 to 80 years (mean  $\pm$  SD,  $65.9 \pm 7.4$  years). The spherical equivalent of their refractive error ranged from  $-4.0$  to  $+3.0$  diopters (D) with a mean of  $-0.6 \pm 1.8$  D. The corrected visual acuity was better than 0.7 in all eyes.

The patients' intraocular pressure (IOP) at the first visit to the clinic ranged from 13 to 19 mmHg with a mean of  $15.9 \pm 1.9$  mmHg in the NTG group, and from 20 to 24 mmHg with a mean of  $21.8 \pm 1.5$  mmHg in the POAG group. Patients with diseases of the anterior segment or retina, dense opacities of the optic media, or a history of ophthalmic surgery were excluded. One 80-year-old patient was

included in the study, as his corrected visual acuity was 1.0 and his senile cataract was incipient.

Disc cupping with a cup/disc ratio  $>0.7$  was present in all subjects. Of the 23 eyes, 22 were receiving antiglaucoma eye drops during the study period. However, none of the subjects were receiving pilocarpine eye drops or oral carbonic anhydrase inhibitor while undergoing mfERG recording, visual field testing, or RNFLT measurement. The IOP at the time of those measurements ranged from 11 to 19 ( $14.5 \pm 2.1$ ) mmHg in the NTG group and from 13 to 16 ( $15.0 \pm 1.2$ ) mmHg in the POAG group.

There were no statistical differences in the mean values of age, refractive error, retinal sensitivity measured by HFA, or s-wave amplitude between the NTG group and the POAG group. Therefore, we analyzed data obtained from eyes with NTG or POAG together.

The subjects were informed of the objectives and methods of the study, and informed consent was obtained from each subject. The procedures were carried out to conform to the tenets of the Declaration of Helsinki.

Because we have already shown that there is a significant difference in the s-wave amplitude between normal eyes and glaucomatous eyes,<sup>3</sup> we have not included data from a normal control group in this study.

### Recording the Multifocal Electoretinogram

Our techniques for recording the mfERG have been described in detail.<sup>1–3</sup> In brief, a visual evoked response imaging system (VERIS; Mayo, Nagoya, Japan) was used to record the mfERG. Before the recording, topical 0.5% tropicamide and 0.5% phenylephrine hydrochloride (Mydrin-P; Santen Pharmaceutical, Osaka, Japan) were used to dilate the test eyes. After about 15 min of light adaptation in a 252-lux room, the surface of the cornea and conjunctiva was anesthetized with 4% lidocaine hydrochloride (Xylocaine; AstraZeneca, Osaka, Japan) and 0.4% oxybuprocaine hydrochloride (Benoxil, Santen).

A bipolar Burian-Allen contact lens-type electrode was placed in the test eye, and the opposite eye was masked. A silver-plated electrode was attached to the right earlobe. The refractive error was measured by an autorefractometer, and a lens with power equal to the spherical equivalent of the refractive error plus 3.0 D was placed in front of the test eye.

The stimulus was composed of 37 hexagonal elements (white or black) arranged in a concentric pattern and displayed on a 17-inch cathode ray tube monitor. The stimulus elements were smallest at the center and increased in size toward the periphery. The overall visual angle of the 37 elements was  $40^\circ$  in the vertical direction and  $50^\circ$  in the horizontal direction. Each stimulus element was reversed from white ( $200 \text{ cd/m}^2$ ) to black ( $4 \text{ cd/m}^2$ ) in a pseudorandom binary m-sequence. The frequency of the reversal was set at 9.4 Hz. A gray element ( $66.6 \text{ cd/m}^2$ ) was interposed between the white and black (or white) elements at 75 Hz (Fig. 1).

Stimulus frequency  
( Hz )

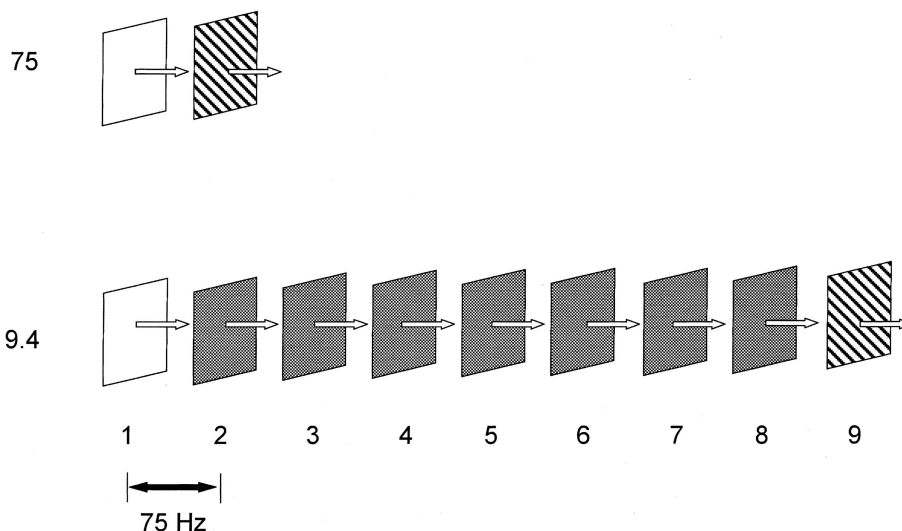


**Figure 1.** Stimulus patterns used by the visual evoked response imaging system to record the multifocal electroretinogram (mfERG) in glaucomatous eyes. Gray elements ( $66.6 \text{ cd/m}^2$ ) were interposed between the white and black (or white) elements at a frequency of 75 Hz. The elements illustrated with striped patterns are white or black according to a pseudorandom binary m-sequence.

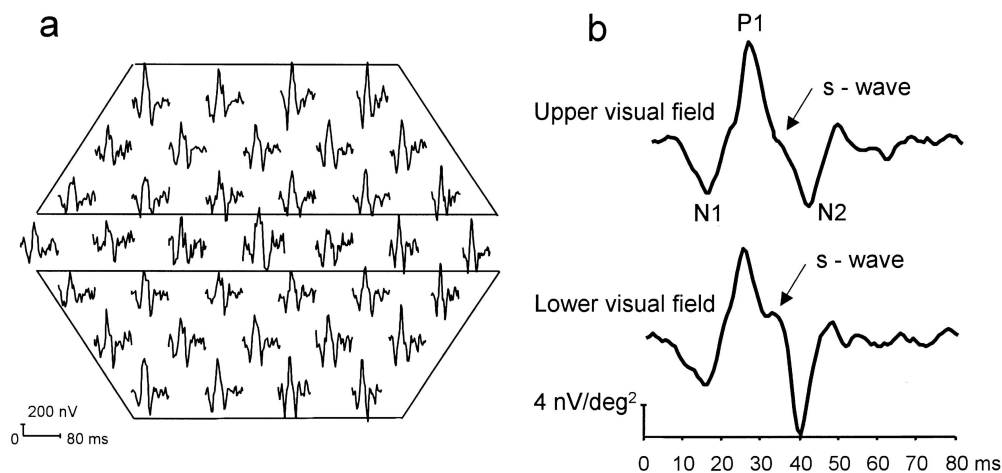


**Figure 2a,b.** mfERG recorded from a glaucomatous eye. **a** All-trace array pattern of 15 responses from the upper and lower halves of the visual field are summed. **b** Representative mfERG waves from summation and averaging of 15 waves from the upper and lower visual fields. The amplitude of the s-wave recorded from the upper visual field (with more severe visual defects) of this eye is smaller than that of the s-wave recorded from the lower visual field (with less severe visual defects). P1, first positive wave; N1, N2, negative waves.

The contrast between the white and gray elements was 50%. The background luminance around the 37 stimulus elements was set at  $40 \text{ cd/m}^2$ . The subject was instructed to fixate on the center of the monitor screen.

Recordings were obtained in eight sessions with 30 s per session for a total recording duration of 4 min. The band-pass filters were set at 10 Hz and 300 Hz, and artifact removal was used once. The mfERGs were analyzed with the VERIS 4.1.1 program (Tomey, Nagoya, Japan).

The first-order kernel of the 37 mfERG recordings was divided into those recorded from the upper and the lower visual field halves. Fifteen patterns from each half visual field were summed and averaged (Fig. 2a) to yield the averaged mfERGs of each half visual field (Fig. 2b). The amplitude and implicit time of the s wave and P1 of the first-order kernel were measured in the 46 averaged mfERGs obtained for the upper and lower visual fields of the 23 eyes.

The amplitude of the s-wave was measured from the apex of the wave peak to the intersection of a vertical line through the apex with a straight line connecting the troughs before and after the s-wave peak. The amplitude of P1 was measured from the lowest point of N1 to the apex of P1. The implicit times of the s-wave and P1 were measured from the onset of the stimulus to the maxima of the wave peaks (Fig. 3).

### Static Perimetry

Static perimetry was performed with an HFA 700 Series instrument (Carl Zeiss Meditec, Dublin, CA, USA), using the Swedish Interactive Threshold Algorithm (SITA), Standard 24-2. The target had the following features: size, III; color, white; and background luminance,  $31.5 \text{ asb}$ .

The percentage of times when the subject was not fixating satisfactorily, the percentage of false-positive responses (button-pushing in the absence of stimulus), and the percentage of false-negatives (not pushing in the presence of a stimulus) were all below 20%. The perimetric data were analyzed separately for the upper and lower halves of the visual field, as was done for the mfERG data (Fig. 4a). The

mean sensitivity (dB) at 26 points within each half of the visual field was averaged (Fig. 4b). Of the 46 visual field halves, those with an MD value  $\leq -5$  dB were placed in group A and those with an MD value  $> -5$  dB were placed in group B. The mean ages in groups A and B were  $67.0 \pm 7.1$  and  $64.7 \pm 7.5$  years, respectively. The mean spherical equivalents of the refractive error in groups A and B were  $-0.5 \pm 1.8$  D and  $-0.5 \pm 1.5$  D, respectively. No statistical difference was found in the mean ages or in the mean spherical equivalents of the refractive error between groups A and B.

### Retinal Nerve Fiber Layer Thickness Measurement with GDx

The RNFLT was measured with the GDx (Laser Diagnostic Technologies, San Diego, CA, USA) without mydriasis. The subject was instructed to place his face on the mask of the GDx and fixate on two flickering horizontal lines within the field of the monitor. The examiner adjusted the location of the test eye and the focus on the monitor. An image ( $256 \times 129$  pixels) for a  $15^\circ \times 15^\circ$  field around the optic nerve head was obtained. The examiner outlined the optic nerve head in the fundus image displayed on the monitor with two circles; an outer circle with a diameter of 1.628 mm and an inner circle with a diameter of 1.256 mm (Fig. 5a). The RNFLT in the annulus was measured. The average RNFLT for the upper  $120^\circ$  (superior average) and lower  $120^\circ$  (inferior average) areas were used in the analyses.

### Measurement with Optical Coherence Tomography

After mydriasis with Mydrin-P, the subject was instructed to fixate on the fixation lamp of the OCT (Carl Zeiss) and an image of his or her optic nerve head was obtained in the

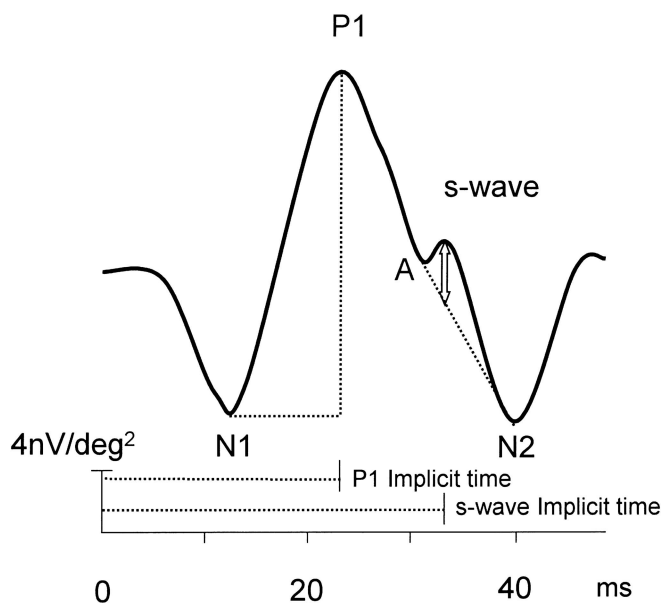


**Figure 3.** Method of measuring the amplitudes and implicit times of the s-wave and P1 of the mfERGs. s-wave: the amplitude of the s-wave was measured from the apex of the peak to the intersection of a vertical line through the apex with a straight line connecting the troughs before and after the s-wave peak. The implicit time of the s-wave was measured from stimulus onset to the apex of the peak of the s-wave. P1: the amplitude of P1 was measured from the trough of N1 to the peak maximum of P1. Implicit time was measured from stimulus onset to the peak of P1.

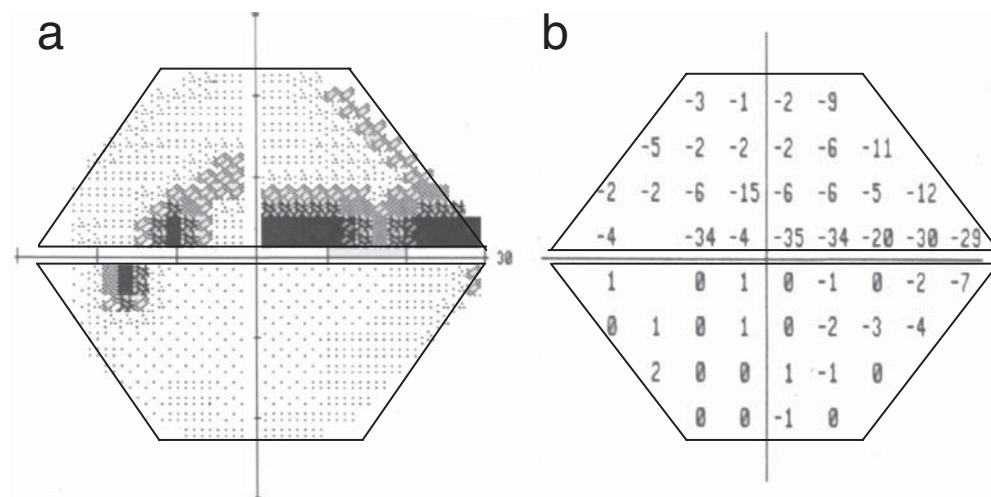
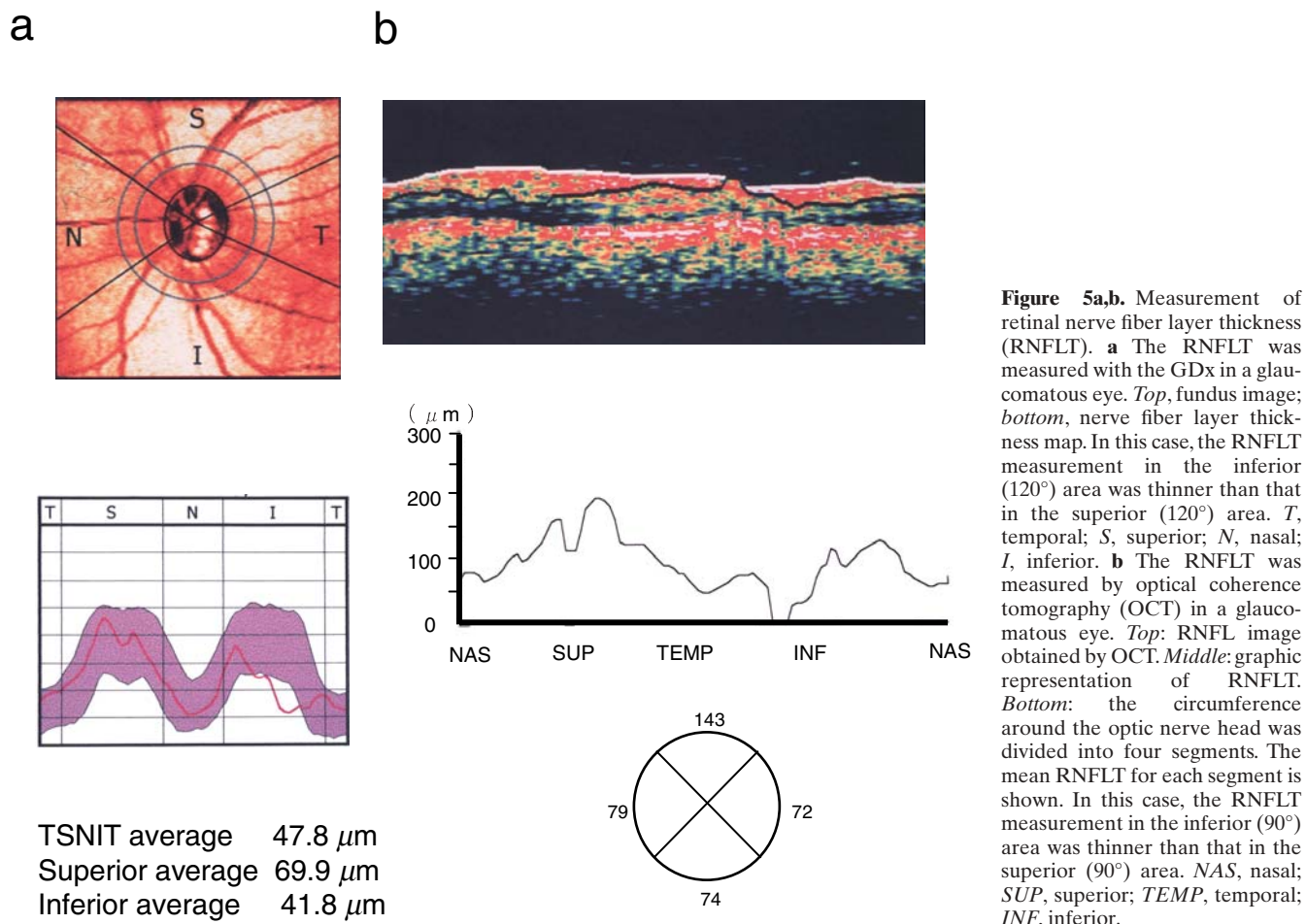


**Figure 4a,b.** Humphrey field analyzer (HFA) data from a glaucomatous eye. **a** HFA data are compiled separately for the upper and lower halves of the visual fields. **b** The mean deviation (MD) measured separately for the upper and lower halves of the visual fields were averaged for each eye.





middle of the video monitor screen. After the image was focused, the area within a radius of 1.73 mm around the optic nerve head was scanned. The fundus tomogram of the left eye was displayed in the following order: nasal, superior, temporal, inferior, and nasal side of the optic nerve head. The circumference around the optic nerve head was divided into four segments (superior, inferior, temporal, and nasal). The mean RNFLT was calculated for each 90° area in the superior and inferior segments (Fig. 5b).

### Statistical Analysis

The relationships among the s-wave, MD value of the HFA, and RNFLT were determined by a simple regression analysis. Welch's *t* test was employed to test the significance of differences of the s-wave amplitude and RNFLT between groups A and B. A *P* value of <0.05 was considered to be statistically significant.

## Results

### Mean Deviation by Humphrey Field Analyzer

The MDs, measured by HFA from the 46 visual field halves, ranged from -28.3 to 1.7 dB with a mean  $\pm$  SD of  $-7.2 \pm 8.3$  dB. In group A (23 halves with a mean MD less than -5.0 dB), the range of MD was -28.3 to -5.1 dB and the mean  $\pm$  SD was  $-13.3 \pm 7.8$  dB. In group B (23 halves with a mean MD higher than -5.0 dB), the corresponding values were -4.6 to 1.7 dB and  $-1.1 \pm 1.8$  dB, respectively. The MD was significantly lower in group A than in group B ( $P < 0.0001$ ) (Table 1).

### Retinal Nerve Fiber Layer Thickness

The RNFLT, measured with the GDx in the 46 visual field halves, ranged from 25.5 to 74.3  $\mu$ m with a mean of  $51.9 \pm 13.2$   $\mu$ m. In group A, the MD ranged from 25.5 to 69.2  $\mu$ m (mean,  $45.5 \pm 11.6$   $\mu$ m), and in group B, it ranged from 38.8 to 74.3  $\mu$ m (mean,  $58.3 \pm 11.7$   $\mu$ m). The RNFLT was significantly thinner in group A than in group B ( $P = 0.0005$ ) (Table 2 and Fig. 6a).

**Table 1.** Grouping of visual field halves by dB values

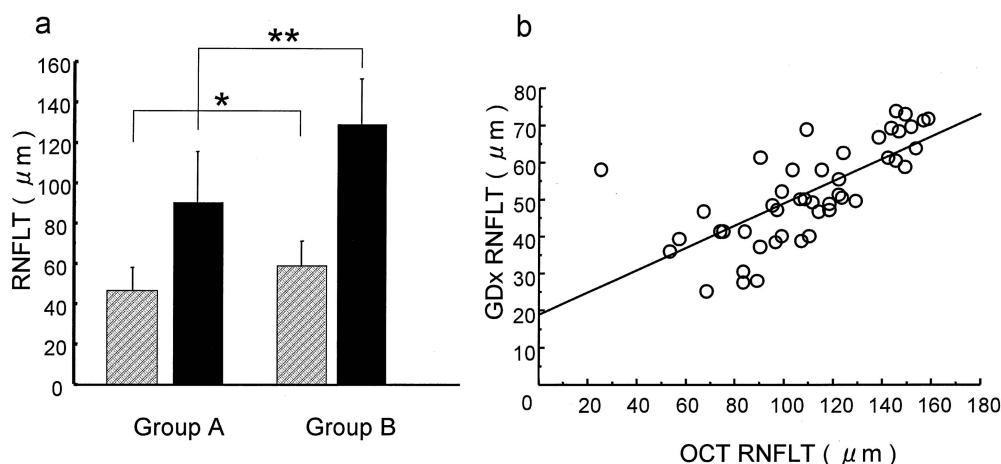
Group	Number of halves	dB	
		Range	Mean $\pm$ SD
A (MD: $\leq -5.0$ dB)	23	-28.3–5.1	-13.3 $\pm$ 7.8
B (MD: $> -5.0$ dB)	23	-4.6–1.7	-1.1 $\pm$ 1.8

MD, mean deviation; SD, standard deviation.

**Table 2.** Retinal nerve fiber layer thickness measured by GDx and OCT

Group	GDx ( $\mu$ m)		OCT ( $\mu$ m)	
	Range	Mean $\pm$ SD	Range	Mean $\pm$ SD
A (MD: $\leq -5.0$ dB)	25.5–69.2	45.5 $\pm$ 11.6	25–149	90.4 $\pm$ 25.7
B (MD: $> -5.0$ dB)	38.8–74.3	58.3 $\pm$ 11.7	67–158	128.7 $\pm$ 22.5

MD, mean deviation; OCT, optical coherence tomography; SD, standard deviation.

**Figure 6a,b.** The retinal nerve fiber layer thickness. **a** RNFLT (mean  $\pm$  SD) measured with the GDx and by OCT in groups A and B. The RNFLT was significantly thinner in group A than in group B. \* $P = 0.001$ ; \*\* $P < 0.0001$ ; ▨, GDx; ■, OCT. **b** Comparison of the RNFLT measurement by OCT and GDx. A decrease in the RNFLT measured by OCT correlated with a decrease in the value measured with the GDx. The correlation between the RNFLT measurements by GDx and OCT is significant ( $y = 0.304x + 18.66$ ,  $r = 0.706$ ,  $P = 0.0009$ ).

The RNFLT, measured by OCT for the 46 visual field halves, ranged from 25 to 158  $\mu$ m with a mean of  $109.5 \pm 30.7 \mu$ m. In group A, the RNFLT ranged from 25 to 149  $\mu$ m (mean,  $90.4 \pm 25.7 \mu$ m), and in group B, it ranged from 67 to 158  $\mu$ m (mean,  $128.7 \pm 22.5 \mu$ m). Thus, the RNFLT was significantly thinner in group A than in group B ( $P < 0.0001$ ; Table 2 and Fig. 6a).

The RNFLT measurements by OCT were significantly thicker than those measured by GDx; however, the RNFLT measurements by OCT significantly correlated with the measurements by GDx ( $r = 0.706$ ,  $P = 0.0009$ ; Fig. 6b).

#### Mean Deviation and Retinal Nerve Fiber Layer Thickness

Lower MD values were associated with significantly thinner RNFLT measurements by GDx ( $r = 0.648$ ,  $P < 0.0001$ ; Fig. 7a). Similarly, lower MD values were associated with significantly thinner RNFLT measurements by OCT ( $r = 0.802$ ,  $P < 0.0001$ ; Fig. 7b).

#### Amplitude of the s-wave of the Multifocal Electroretinogram

Examples of the all-trace mfERGs obtained by summing and averaging the 15 waves from the upper and lower visual field halves of the first-order kernel obtained at 9.4 Hz are shown in Fig. 2b. The amplitude of the s-wave in this patient was smaller in the upper half of the visual field than in the lower half, which corresponded to the more severe alteration in the upper versus the lower visual field as determined by HFA. The amplitude of the s-wave in the all-trace waves obtained from the 46 visual field halves ranged from 2.1 to 5.6 nV/deg<sup>2</sup> with a mean of  $3.5 \pm 0.9$  nV/deg<sup>2</sup>.

#### Correlation Between s-wave Amplitude and Mean Deviation

In group A, the s-wave amplitude ranged from 2.1 to 4.6 nV/deg<sup>2</sup> with a mean of  $2.9 \pm 0.6$  nV/deg<sup>2</sup>, and it ranged from 2.8 to 5.6 nV/deg<sup>2</sup> with a mean of  $4.1 \pm 0.7$  nV/deg<sup>2</sup> in

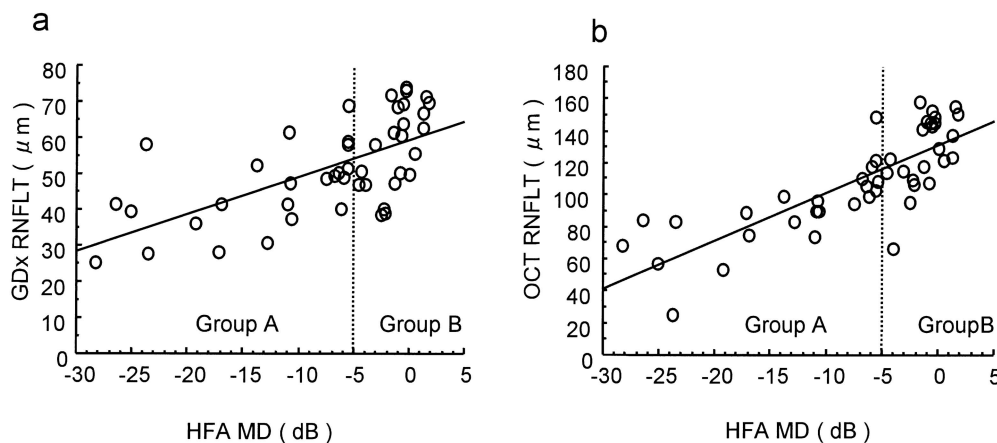


**Figure 7a,b.** Relationship between the MD as measured by HFA and the RNFLT as measured with the GDx (a) and OCT (b). The RNFLT is thinner when the MD values are smaller; the correlation between the RNFLT and the MD values is significant ( $y = 1.034x + 59.357$ ,  $r = 0.648$  for GDx, and  $y = 2.974x + 130.926$ ,  $r = 0.802$  for GDx,  $P < 0.0001$  for OCT).

**Table 3.** Amplitudes and implicit times of s-wave and P1

Wave	Grouping	Amplitude (nV/deg <sup>2</sup> )		Implicit Time (ms)	
		Range	Mean $\pm$ SD	Range	Mean $\pm$ SD
s-wave	A (MD: $\leq -5.0$ dB)	2.1–4.6	$2.9 \pm 0.6$	31.7–37.5	$34.1 \pm 1.6$
	B (MD: $> -5.0$ dB)	2.8–5.6	$4.1 \pm 0.7$	30.8–37.5	$34.2 \pm 1.7$
P1	A (MD: $\leq -5.0$ dB)	13.0–18.4	$15.6 \pm 1.2$	23.2–29.2	$26.1 \pm 1.3$
	B (MD: $> -5.0$ dB)	14.0–18.4	$15.9 \pm 1.3$	24.2–27.5	$25.5 \pm 1.0$

MD, mean deviation; SD, standard deviation.

group B. The mean s-wave amplitude was significantly smaller in group A than in group B ( $P < 0.0001$ ; Table 3 and Fig. 8a).

The relationship between the s-wave amplitude and the MD is shown in Fig. 8b. A lower MD was associated with a smaller amplitude s-wave, and the correlation between these two parameters was significant ( $r = 0.669$ ,  $P < 0.0001$ ).

### Correlation Between s-wave Amplitude and Retinal Nerve Fiber Layer Thickness

A plot of the s-wave amplitude against the RNFLT showed that the s-wave amplitude decreased as the RNFLT, measured with the GDx, became smaller ( $r = 0.535$ ,  $P = 0.0004$ ; Fig. 9a). The s-wave amplitude also significantly correlated with the RNFLT measured by OCT ( $r = 0.682$ ,  $P = 0.0002$ ; Fig. 9b).

### Amplitude of P1 in the Multifocal Electrophoretogram

The amplitude of P1 in group A did not differ significantly from that in group B. There was no significant correlation between the P1 amplitude and the MD, or between the P1 amplitude and the RNFLT (Table 3).

### Implicit Time of s-wave and P1 in the Multifocal Electrophoretogram

No significant difference was found in the implicit times of the s-wave or P1 between groups A and B. There was no significant correlation between the MD and the implicit times of the s-wave or P1. The RNFLT also did not correlate with the implicit times of the s-wave or P1 (Table 3).

## Discussion

Since the technique was first described by Sutter et al.,<sup>4,7</sup> mfERG has been extensively used for clinical diagnosis and research. Various studies have also been conducted to determine the origin of each wave constituting the mfERG. A number of studies have shown that mfERGs reflect the function of not only the outer retinal layers but also the inner retinal layers.<sup>4–9</sup>

The results of our earlier studies have shown that the s-wave is related to the neural activity of retinal ganglion cells and their axons. Thus, we hypothesized that the s-wave would be altered in glaucomatous eyes in which the RGCs are known to be affected from an early stage of the disease. Because it is well known that the RNFLT is thinner in glaucomatous eyes than in normal eyes, and that the degree of

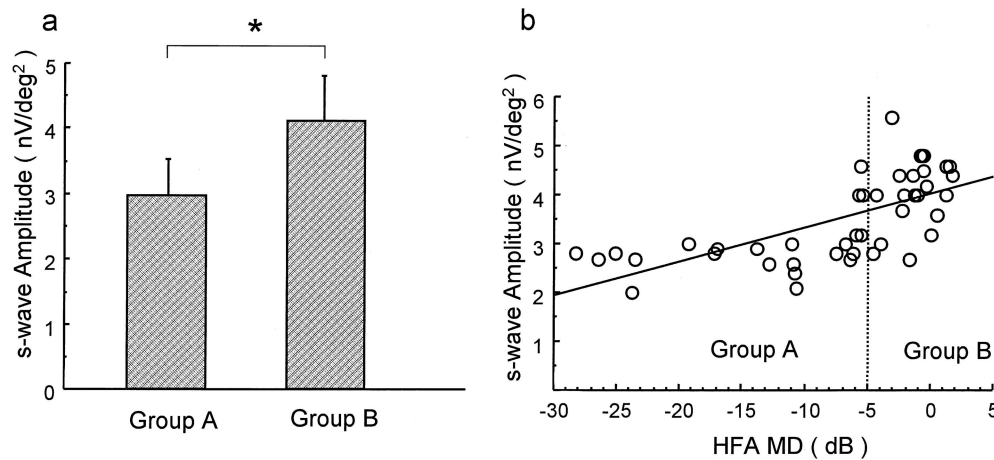


**Figure 8a,b.** The s-wave amplitude (mean  $\pm$  SD) in groups A and B. **a** The s-wave amplitude is significantly smaller in group A than in group B ( $P < 0.0001$ ). **b** Relationship between the s-wave amplitude and MD. The s-wave amplitude is smaller when the value of MD is smaller, and the correlation between the s-wave amplitude and the MD values is significant ( $y = 0.07x + 4.023$ ,  $r = 0.669$ ,  $P < 0.0001$ ).

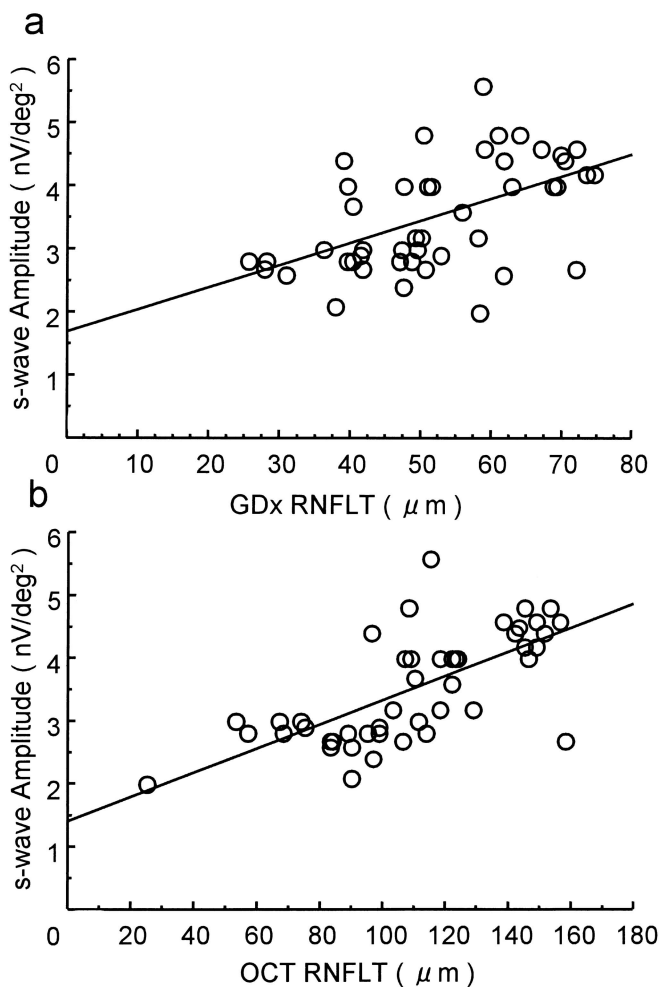


**Figure 9a,b.** Relationship between the s-wave amplitude and the RNFLT. **a** The s-wave amplitude is smaller in eyes with thinner RNFLT when measured by GDx. The correlation between the s-wave amplitude and RNFLT measured by GDx is significant ( $y = 0.035x + 1.699$ ,  $r = 0.535$ ,  $P = 0.0004$ ). **b** Relationship between the RNFLT and the s-wave amplitude when measured by OCT. The s-wave amplitude is smaller in eyes with thinner RNFLT. The correlation between the s-wave amplitude and RNFLT measured by OCT is significant ( $y = 0.019x + 1.413$ ,  $r = 0.682$ ,  $P = 0.0002$ ).

its thinning is correlated with the severity of the visual field defects,<sup>10–12</sup> we hypothesized that the s-wave amplitude would correlate with the RNFLT.

In our previous study, the s-wave was most pronounced at a stimulus frequency under 9.4 Hz.<sup>1–3</sup> However, because the s-wave was much more contaminated with noise when it was recorded at a frequency lower than 9.4 Hz, we used 9.4 Hz in the present study. The mfERG recording time was increased from 2 min to 4 min, resulting in a twofold increase in the number of summations. In this way, mfERGs were recorded with less noise and the s-waves were more prominent. On the basis of these results, we suggest that mfERGs recorded for 4 min at a frequency of 9.4 Hz would be optimal for obtaining the s-wave in clinical cases.

The GDx was used to measure the RNFLT, and its sensitivity and specificity for measuring the RNFLT were 80.9% and 66.7%, respectively.<sup>13</sup> A comparison of the RNFLT of normal eyes measured with the GDx with that of eyes with POAG or NTG, which had glaucomatous disc cupping but had not developed visual field defects, showed that the RNFLT was significantly thinner in the glaucomatous eyes than in the normal eyes.<sup>12</sup> A significant correlation between the RNFLT as measured with the GDx and the amplitude of the pattern ERG has been reported.<sup>14</sup>

The RNFLT measured by OCT has been shown to correlate with the MD of the visual field.<sup>10</sup> Thus, OCT was reported to be useful for the diagnosis of glaucomatous neuropathy.<sup>15–23</sup> The mean RNFLT measured by OCT in normal eyes, suspected glaucomatous eyes, and eyes with early stage glaucoma were reported as  $128.4 \pm 15.4$ ,  $102.0 \pm 25.4$ , and  $86.5 \pm 31.5 \mu$ m, respectively.<sup>22</sup> The RNFLT obtained in the glaucomatous eyes by OCT in the present study are consistent with these values.

Our RNFLT measurements by OCT were significantly thicker than those measured by GDx. This is in good agreement with previous studies,<sup>11,16</sup> although Furuichi et al.<sup>11</sup> reported that the RNFLT measurement of only the superior quadrant was significantly greater when measured by OCT than when measured by scanning laser polarimeter. Hoh et al.,<sup>16</sup> on the other hand, reported a significant correlation between RNFLT measurements by OCT and GDx.



We also found that the RNFLT measurements with the GDx significantly correlated with those obtained by OCT, consistent with the observations reported by Hoh et al.<sup>16</sup> The reason for the differences in the mean values of the RNFLT measurements with the GDx and by OCT has not been determined. In any case, we conclude that both the GDx and OCT are suitable for evaluation of the RNFLT in glaucomatous eyes.

Many clinical and experimental studies have been reported concerning the mfERG waves in glaucomatous eyes.<sup>2,3,6,24–33</sup> One study reported that the amplitudes of the N1, P1, and N2 of the first-order kernel of the mfERG were smaller and the implicit times were longer in glaucomatous eyes than in normal eyes, but that none of these parameters showed any correlation with the MD as measured by perimetry.<sup>25</sup> On the other hand, another study showed that the MD measurement by perimetry correlated with the amplitude of the P1 and N2 of the first-order kernel responses.<sup>31</sup> Hood et al.<sup>6</sup> evaluated the severity of visual field defects in POAG eyes and the amplitude ratio of the two positive waves seen in the first-order kernel of the mfERG. They reported that the amplitude ratio was smaller in glaucomatous eyes than in normal eyes, although the severity of the visual field defects did not significantly correlate with the amplitude ratio. Furthermore, Hood et al.<sup>6</sup> experimentally induced nerve fiber layer bundle defects around the optic nerve head of monkey eyes by laser photocoagulation<sup>34</sup> and subsequently recorded the mfERG, using three methods of stimulation: standard fast m-sequence flicker, full-field flashes, and slowed m-sequence, with seven dark frames inserted in each m-step (7F). They reported that localized RGC damage could be detected more clearly with the 7F m-sequence stimulation than by the other two methods, and they concluded that the slowed m-sequence mfERG is the most suitable for evaluating RGC function.<sup>34</sup>

Some investigators have analyzed HFA data from glaucomatous eyes separately for the upper and lower visual field halves, and they have analyzed the relationship between the MD in each visual field half and the amplitude of P1 and N1 in the mfERG in the corresponding visual field half. They found that the correlations between the MD and the amplitude of P1 and N1 in the mfERG were not significant.<sup>24</sup> Palmowski et al.<sup>35</sup> divided the visual field of each glaucomatous eye into four segments and analyzed the relationship between the MD and amplitude of the N1, P1, and N2 of the mfERGs for each segment. They also found no significant correlation between the MD and the amplitude of the waves in the mfERG.

We previously studied the relationship between the severity of visual field defects and the s-wave amplitude in normal eyes and glaucomatous eyes.<sup>3</sup> As mentioned earlier, our results showed a significantly smaller s-wave amplitude in glaucomatous eyes than in normal eyes.<sup>2</sup> Furthermore, a significant correlation was found between the severity of the visual field defects and the s-wave amplitude in glaucomatous eyes.<sup>3</sup> The mean s-wave amplitude in the present study, even in group A, was smaller than that in normal eyes mea-

sured in our previous studies.<sup>2,3</sup> The correlation between the s-wave amplitude and the visual field defects supports our earlier findings. In addition, the strong correlation between the RNFLT and the s-wave amplitude, that is, the amplitude of the s-wave significantly decreased as the RNFLT became smaller, further supports our hypothesis that the s-wave reflects the function of the RGCs and their axons.

At present, there are few methods available clinically for the objective evaluation of the functions of the RGC layers and their axons. Analysis of the s-wave as an indicator of this function therefore appears promising for early detection, diagnosis, and follow-up of glaucoma and other diseases associated with damage to the RGC layers and their axons.

## References

1. Sano M, Tazawa Y, Nabeshima T, Mita M. A new wavelet in the multifocal electroretinogram, probably originating from ganglion cells. *Invest Ophthalmol Vis Sci* 2002;43:1666–1672.
2. Kobayashi M, Tazawa Y, Haga-Sano M, Nabeshima T, Murai K. Changes in s-wave of multifocal electroretinograms in eyes with primary open-angle glaucoma. *Jpn J Ophthalmol* 2004;48:208–214.
3. Murai K, Tazawa Y, Kobayashi M, Hayasaka A. Amplitude of the s-wave of multifocal electroretinograms can indicate local retinal sensitivity in glaucomatous eyes. *Jpn J Ophthalmol* 2004;48:215–221.
4. Sutter EE, Bearse MA. The optic nerve head component of the human ERG. *Vision Res* 1999;39:419–436.
5. Hood DC, Bearse MA, Sutter EE, Viswanathan S, Frishman LJ. The optic nerve head component of the monkey's (*Macaca mulatta*) multifocal electroretinogram (mERG). *Vision Res* 2001;41:2029–2041.
6. Hood DC, Greenstein VC, Holopigian K, et al. An attempt to detect glaucomatous damage to the inner retina with the multifocal ERG. *Invest Ophthalmol Vis Sci* 2000;41:1570–1579.
7. Sutter EE, Tran D. The field topography of ERG components in man. I. The photopic luminance response. *Vision Res* 1992;32:433–446.
8. Hood DC, Frishman LJ, Viswanathan S, Robson JG, Ahmed J. Evidence for a ganglion cell contribution to the primate electroretinogram (ERG): Effect of TTX on the multifocal ERG in macaque. *Vis Neurosci* 1999;16:411–416.
9. Hood DC, Greenstein V, Frishman L, et al. Identifying inner retinal contribution to the human multifocal ERG. *Vision Res* 1999;39:2285–2291.
10. Schuman JS, Hee MR, Puliafito CA, et al. Quantification of nerve fiber layer thickness in normal and glaucomatous eyes using optical coherence tomography: a pilot study. *Arch Ophthalmol* 1995;113:586–596.
11. Furuichi M, Kashiwagi K, Furuichi Y, Tsukahara S. Comparison of the effectiveness of scanning laser polarimetry and optical coherence tomography for estimating optic nerve fibre layer thickness in patients with glaucoma. *Ophthalmologica* 2002;216:168–174.
12. Matsumoto C, Shirato S, Haneda M, Yamashiro H, Saito M. Study of retinal nerve fiber layer thickness within normal hemivisual field in primary open-angle glaucoma and normal-tension glaucoma. *Jpn J Ophthalmol* 2003;47:22–27.
13. Funaki S, Shirakashi M, Yaoeda K, et al. Specificity and sensitivity of glaucoma detection in the Japanese population using scanning laser polarimetry. *Br J Ophthalmol* 2002;86:70–74.
14. Toffli G, Vattovani O, Cecchini P, et al. Correlation between the retinal nerve fiber layer thickness and pattern electroretinogram amplitude. *Ophthalmologica* 2002;216:159–163.

15. Bowd C, Weinreb RN, Williams JM, et al. The retinal nerve fiber layer thickness in ocular hypertensive, normal, and glaucomatous eyes with optical coherence tomography. *Arch Ophthalmol* 2000; 118:22–26.
16. Hoh ST, Greenfield DS, Mistlberger A, et al. Optical coherence tomography and scanning laser polarimetry in normal, ocular hypertensive, and glaucomatous eyes. *Am J Ophthalmol* 2000; 129:129–135.
17. Zangwill LM, Bowd C, Berry CC, et al. Discriminating between normal and glaucomatous eyes using the Heidelberg retina tomograph, GDx nerve fiber analyzer, and optical coherence tomograph. *Arch Ophthalmol* 2001;119:985–993.
18. Bowd C, Zangwill LM, Berry CC, et al. Detecting early glaucoma by assessment of retinal nerve fiber layer thickness and visual function. *Invest Ophthalmol Vis Sci* 2001;42:1993–2003.
19. Soliman MAE, Van Den Berg TJTP, Ismaeil AA, et al. Retinal nerve fiber layer analysis: relationship between optical coherence tomography and red-free photography. *Am J Ophthalmol* 2002; 133:187–195.
20. El Beltagi TA, Bowd C, Boden C, et al. Retinal nerve fiber layer thickness measured with optical coherence tomography is related to visual function in glaucomatous eyes. *Ophthalmology* 2003;110: 2185–2191.
21. Jaffe GJ, Caprioli J. Optical coherence tomography to detect and manage retinal disease and glaucoma. *Am J Ophthalmol* 2004;137: 156–169.
22. Nouri-Mahdavi K, Hoffman D, Tannenbaum DP, et al. Identifying early glaucoma with optical coherence tomography. *Am J Ophthalmol* 2004;137:228–235.
23. Bagga H, Greenfield DS. Quantitative assessment of structural damage in eyes with localized visual field abnormalities. *Am J Ophthalmol* 2004;137:797–805.
24. Satomi A, Sano N, Kawabata H, Adachi-Usami E. Use of multifocal electroretinography to evaluate eyes with glaucoma. *Nihon Ganka Kiyo (Folia Ophthalmol Jpn)* 1997;48:583–587.
25. Okano M, Nao-i N, Arai M, et al. Multifocal electroretinogram in eyes with glaucoma. *Nihon Ganka Kiyo (Folia Ophthalmol Jpn)* 1999;50:443–448.
26. Chan HL, Brown B. Multifocal ERG changes in glaucoma. *Ophthalmic Physiol Opt* 1999;4:306–316.
27. Hare W, Ton H, Woldemussie E, et al. Electrophysiological and histological measures of retinal injury in chronic ocular hypertensive monkeys. *Eur J Ophthalmol* 1999;9:30–33.
28. Hasegawa S, Takagi M, Usui T, Takada R, Abe H. Waveform changes of the first-order multifocal electroretinogram in patient with glaucoma. *Invest Ophthalmol Vis Sci* 2000;41:1597–1603.
29. Palmowski AM, Allgayer R, Heinemann-Vemaleken B. The multifocal ERG in open angle glaucoma: a comparison of high and low contrast recordings in high- and low-tension open angle glaucoma. *Doc Ophthalmol* 2000;101:35–49.
30. Frishman LJ, Saszik S, Harwerth RS, et al. Effects of experimental glaucoma in macaques on the multifocal ERG. Multifocal ERG in laser-induced glaucoma. *Doc Ophthalmol* 2000;100:231–251.
31. Ito M, Murayama K, Kanno J, Yoneya S. Usefulness of multifocal electroretinograms in detecting visual dysfunction in eyes with glaucoma. *Nihon Ganka Kiyo (Folia Ophthalmol Jpn)* 2000;51: 746–753.
32. Raz D, Seelinger MW, Geva AB, et al. The effect of contrast and luminance on mfERG responses in a monkey model of glaucoma. *Invest Ophthalmol Vis Sci* 2002;43:2027–2035.
33. Fortune B, Bearnse MA, Cioffi GA, Johnson CA. Selective loss of an oscillatory component from temporal retinal multifocal ERG responses in glaucoma. *Invest Ophthalmol Vis Sci* 2002;43:2638–2647.
34. Fortune B, Wang L, Bui BG, et al. Local ganglion cell contributions to the macaque electroretinogram revealed by experimental nerve fiber bundle defect. *Invest Ophthalmol Vis Sci* 2003;44:4567–4579.
35. Palmowski MA, Ruprecht WK. Follow up in open angle glaucoma. A comparison of static perimetry and the fast stimulation mfERG. *Doc Ophthalmol* 2004;108:55–60.